^{31}P-NMR study of hyperfine interactions and magnetic fluctuations in the neptunium-based filled skutterudite $NpFe_4P_{12}$

Y. Tokunaga,* S. Kambe, H. Sakai, H. Chudo, T. D. Matsuda, Y. Haga, and H. Yasuoka
ASRC, Japan Atomic Energy Agency, Tokai, Ibaraki 319-1195, Japan

D. Aoki,† Y. Homma, and Y. Shiokawa
IMR Tohoku University, 2145-2 Narita Oarai Higashiibaraki, Ibaraki 311-1313, Japan

Y. Ōnuki
Graduate School of Science, Osaka University, 1-1 Machikaneyama-cho, Toyonaka, Osaka 560-0043, Japan and ASRC, Japan Atomic Energy Agency, Tokai, Ibaraki 319-1195, Japan

(Received 11 September 2008; published 18 February 2009)

^{31}P-NMR measurements have been performed on a single crystal of the neptunium-based filled skutterudite $NpFe_4P_{12}$. The compound undergoes a ferromagnetic phase transition at T_C=23 K. From the field-orientation dependence of the ^{31}P-NMR line splitting, the angular dependence of the hyperfine interactions between Np 5*f* spin and ^{31}P nuclear moments has been investigated. We have observed anisotropic transferred hyperfine interactions at the P sites, which lead to an estimate of the local spin density in the P 3*p* orbitals. It is shown that a fraction of the Np 5*f* spin moments is transferred mostly into the P 3*p* orbitals extending toward the inside of a P cage. The weak hybridization between Np 5*f* and P 3*p* orbitals suggests a localized character for Np 5*f* electrons in $NpFe_4P_{12}$. We have also measured the field and temperature dependences of the nuclear spin-lattice relaxation rate $(1/T_1)$ in several magnetic fields between 18.5 and 78.0 kOe. The $1/T_1$ data reveal that the low-energy spin fluctuations of Np 5*f* spin moments are strongly suppressed by applied fields over a relatively wide temperature range up to $4T_C$. In this compound, a large and negative magnetoresistance has been known to occur in the same temperature range. The present NMR results demonstrate that the negative magnetoresistance comes from a reduction in the magnetic scattering from Np 5*f* spin moments by an applied field.

DOI: 10.1103/PhysRevB.79.054420 PACS number(s): 76.60.−k, 75.50.Dd, 71.27.+a

I. INTRODUCTION

Compounds with the filled skutterudite structure RT_4X_{12} (R=rare earth or actinide, T=transition metal, X=pnictogen) exhibit a variety of exotic phenomena in a common crystal structure.[1,2] Most of the exotic phenomena are thought to originate in their unique crystal structure: the large coordination number of R ions surrounded by a 12 X-ion cage leads to a relatively large hybridization effect between conduction electrons and f electrons (Fig. 1). The replacement of T and X ions yields variations in the lattice constant, which result in variations in the degree of the c-f hybridization.

Recently, Aoki *et al.*[3] have discovered a unique filled skutterudite $NpFe_4P_{12}$. This is a filled skutterudite which incorporates a transuranium element. The lattice constant was determined to be 7.7702(7) Å, which is the smallest value of all the filled skutterudites. Magnetization measurements revealed the compound to be a ferromagnet with a Curie temperature T_C=23 K. The T_C value is nearly an order-of-magnitude higher than those for UFe_4P_{12} (T_c=3.1 K) (Refs. 4–6) and $NdFe_4P_{12}$ (1.9 K).[7–9] The ferromagnetic easy axes were determined to be directed along the ⟨100⟩ direction with a saturated moment of $1.35\mu_B$/Np.[3,10]

On the other hand, the resistivity exhibits a peculiar temperature dependence, that is, it increases rapidly below 150 K and shows a broad maximum around 30 K. Based on its large resistivity value in the whole temperature region, the compound is suggested to be a semimetal, where the Np 5*f* electron is localized and a $5f^3(Np^{4+})$ configuration is realized. Another remarkable feature of the transport is the negative magnetoresistance (MR) observed in a wide temperature range of up to 80 K (about four times T_C). A change in resistance induced by a magnetic field has been found to

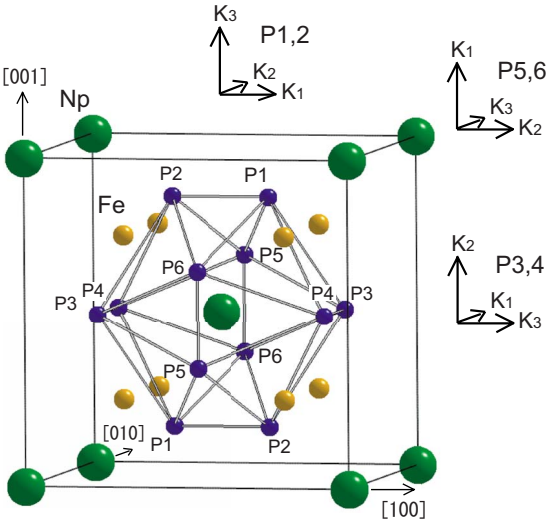

FIG. 1. (Color online) Schematic view of the crystal structure of $NpFe_4P_{12}$. The P cages surrounding the corner Np atoms are omitted for clarity. Arrows show the definition of principal axes for the Knight-shift tensors at P sites.

reach an enormous value (about −60%) around 30 K. Note that similar negative MR effects have been reported in UFe_4P_{12} (Refs. 4–6) and $NdFe_4P_{12}$,[7,9] suggesting that a common mechanism for the negative MR may exist in these isomorphic ferromagnets.

In this paper, we report ^{31}P-NMR measurements performed on a single crystal of $NpFe_4P_{12}$. The advantage of NMR experiments is that microscopic properties can be selectively probed for each site in a given compound. In this study, we focus on the electronic state of the P-cage characteristic of the filled skutterudites. We extract the temperature and the field-orientation dependences of the transferred hyperfine (HF) interactions, and deduce the local spin density at P 3*p* orbitals. It is shown that, due to the orbital hybridization effect, a fraction of the Np 5*f* spin moment is transferred into the P 3*p* orbitals extending toward the inside of the P cage.

In the latter half of the paper, we report the field and temperature dependence of the nuclear spin-lattice relaxation rate $(1/T_1)$ at the P sites. The $1/T_1$ data reveal that ferromagnetic fluctuations are strongly suppressed by applied fields in a relatively wide temperature region below 100 K. This result demonstrates that the large negative MR effect which occurs in the same temperature region comes from the reduction in magnetic scattering from Np local moments by an applied field.

II. EXPERIMENTAL

Single crystals of $NpFe_4P_{12}$ were grown by a Sn-flux method described in detail elsewhere.[3] The ^{31}P-NMR measurements were carried out using a superconducting magnet and a phase-coherent pulsed spectrometer. To minimize a possible perturbation due to the field-orientation dependence of the demagnetization effect, a single crystal with a spherical shape has been selected. The temperature and field angle dependences of the NMR line shift were measured on a single crystal mounted on a two-axis sample rotator. The spin-lattice relaxation time T_1 was measured on the same single crystal, using the saturation-recovery method in several fields between 18.5 and 78.0 kOe. Nuclear magnetization recovery was found to fit a simple exponential for these $I=1/2$ nuclei, allowing us to determine a unique T_1 value at each temperature and field.

III. EXPERIMENTAL RESULTS AND DISCUSSION

A. Angular dependence of the HF interactions

Figure 2 shows the field-orientation dependence of ^{31}P-NMR spectra obtained at 100 K with an applied magnetic field $H_0=46.55$ kOe. Here, θ is the polar angle of $\mathbf{H}_0$ relative to the [001] axis of the crystal, and $\mathbf{H}_0$ rotates through the [111] to the [110] directions so that the applied field is given by $\mathbf{H}_0=(H_x,H_y,H_z)=\frac{H_0}{\sqrt{2}}(\sin\theta,\sin\theta,\sqrt{2}\cos\theta)$. In $NpFe_4P_{12}$, there are twelve P atoms forming an icosahedral cage surrounding a Np atom, as illustrated in Fig. 1. They are all crystallographically equivalent in a cubic unit cell. However, since the local symmetry at each P site is lower than cubic, a distribution of anisotropic HF interactions causes a splitting of ^{31}P-NMR line under external magnetic field.[11,12] As seen in Fig. 2, the NMR line splits into several peaks (six at the maximum) and these peaks change their position with sample rotation. For later discussion, we label the six P sites giving different NMR peaks as P1–P6 (see Fig. 1).

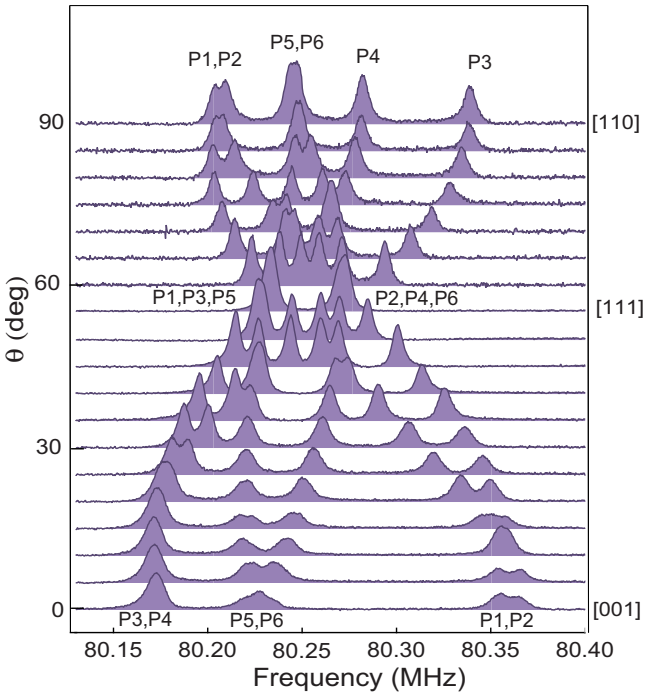

FIG. 2. (Color online) The field-orientation dependence of the ^{31}P-NMR spectra at 100 K with an applied field $H_0=4.655$ T. θ indicates the angle of tilt for the field as it rotates from ⟨001⟩ to ⟨110⟩ through ⟨111⟩ directions of the $NpFe_4P_{12}$ crystal.

In Fig. 3(a), we plot the angular dependence of the NMR line splitting $\Delta H=(f_{\rm res}-f_0)/\gamma$, where $f_{\rm res}$ is the center of gravity of one of the observed NMR peaks, $f_0=\gamma\cdot\mathbf{H}_0$, and $\gamma=17.237$ MHz/T for ^{31}P nuclei. A series of six curves merges into four, three, and then two along the [110], [001], and [111] directions, respectively. Note that the observed NMR line splittings are of purely magnetic origin since the ^{31}P nuclei $(I=1/2)$ have no electric-quadrupole moment. The demagnetization effect at this temperature has been estimated to be ~3 Oe, which is an order-of-magnitude smaller than ΔH. Therefore, the angular dependence of ΔH in Fig. 3(a) corresponds to the angular dependence of the HF field over the P sites. Since the magnetic susceptibility χ of $NpFe_4P_{12}$ is isotropic, the anisotropic character of the HF field indicates that the HF coupling mechanism itself is anisotropic.

In filled skutterudites, the P nuclei can be regarded as belonging to ligand sites, which have no intrinsic magnetic moment. The nuclear-spin Hamiltonian of ^{31}P may be written using the second-rank Knight-shift tensor $\mathbf{K}$ as

$$\mathcal{H}=-\gamma_N\hbar\mathbf{I}\cdot\mathbf{H}_0-\gamma_N\hbar\mathbf{I}\cdot\mathbf{H}_{\rm dip}-\gamma_N\hbar[\mathbf{I}\cdot\mathbf{K}\cdot\mathbf{H}_0], \quad (1)$$

where the first term is due to the Zeeman interaction between the nuclear spin $\mathbf{I}$ and the applied field $\mathbf{H}_0$. The second term

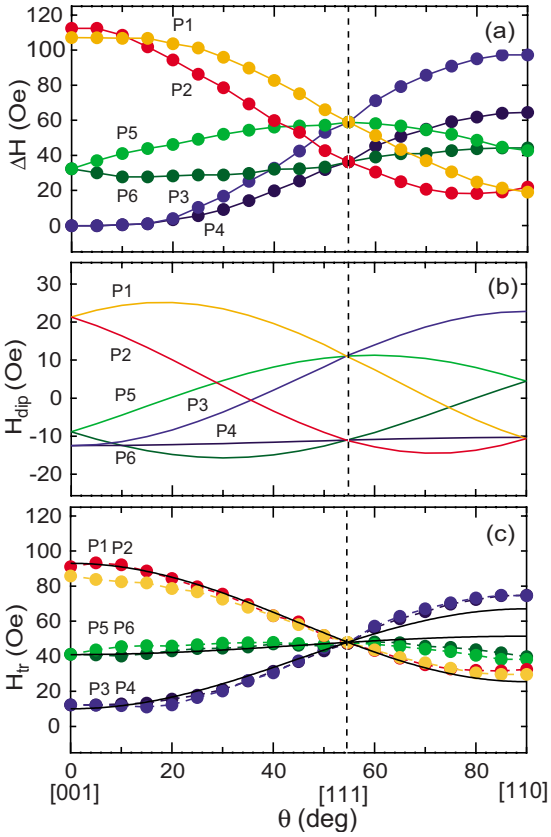

FIG. 3. (Color online) (a) The angular dependence of the NMR line splitting $\Delta H=(f_{\rm res}-f_0)/\gamma$, where $f_{\rm res}$ is the center of gravity of one of the observed NMR peaks, $f_0=\gamma\cdot\mathbf{H}_0$, and $\gamma=17.237$ MHz/T for ^{31}P nuclei. (b) The angular dependence of the dipolar field $H_{\rm dip}$ calculated assuming localized moments of $\bar{\mu}_j=0.044\mu_B$ along the field direction located on the Np sites. (c) The angular dependence of the transferred HF field $H_{\rm tr}$ obtained by subtracting the $H_{\rm dip}$ from the ΔH. The solid lines are the calculated curves of Eqs. (3)–(5) with $K_{\rm iso}H_0=48$ Oe and $(K_1,K_2,K_3)H_0=(-38,-7,45)$ Oe, respectively.

is the classical dipolar interaction arising from Np $5f$ local moments. The third term is the so-called transferred HF interaction arising from the on-site spin density at P sites as a consequence of the orbital hybridization effect between Np $5f$ and P $3p(3s)$ electrons.

The dipolar field from the Np spin moment at site j to the ^{31}P nucleus at site i can be calculated as

$$H_{\rm dip}(ij)=\left[3\frac{\bar{\mu}_j\cdot\vec{r}_{ij}}{r_{ij}^5}-\frac{\bar{\mu}_j}{r_{ij}^3}\right], \tag{2}$$

where $\bar{\mu}_j$ is the time average $5f$ spin moment along $\mathbf{H}_0$. Using Eq. (1), the dipolar field at a ^{31}P site is obtained by summing over all of the Np moments in the crystal. The solid lines in Fig. 3(b) show the calculated angular dependence of $H_{\rm dip}$ with the value of $\bar{\mu}_j=0.044\mu_B$ estimated from magnetization measurements at $T=100$ K. We have obtained a series of six curves with a θ dependence which is analogous to the θ dependence of ΔH. Quantitatively, however, the latter dipolar calculation gives an NMR line splitting about one-third of the magnitude of ΔH, as shown in Figs. 3(a) and 3(b).

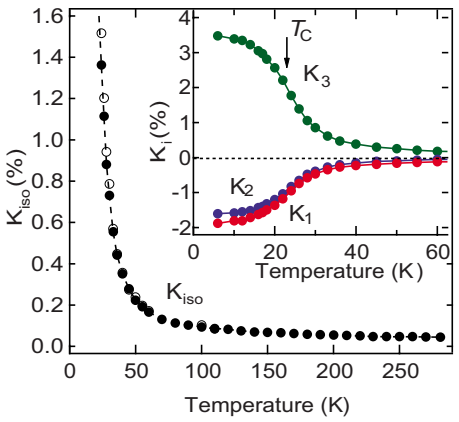

FIG. 4. (Color online) The temperature dependence of the isotropic and anisotropic parts of the Knight shift $K_{\rm iso}$ and K_i ($i=1$, 2 and 3).

This result indicates that another HF mechanism, i.e., the transferred HF mechanism, occurs here with a magnitude similar to that of the direct dipolar mechanism.

Figure 3(c) shows the angular dependence of the transferred HF field $H_{\rm tr}$ obtained by subtracting the dipole contribution $H_{\rm dip}$ from ΔH as $H_{\rm tr}=\Delta H-H_{\rm dip}$. We found that the six curves for ΔH merge into three curves for $H_{\rm tr}$. This reveals that the neighboring P sites, P1–P2, P3–P4, and P5–P6 sites, are pairwise equivalent regarding $H_{\rm tr}$. These results are consistent with the assumption that the anisotropic components of $H_{\rm tr}$ arises from the anisotropic hyperfine interactions with the on-site spin density of P $3p$ orbitals. When the bulk susceptibility $\chi(T)$ is isotropic, the θ dependence of $H_{\rm tr}$ over the P sites can be reproduced by using a second-rank Knight-shift tensor consisting of an isotropic term $K_{\rm iso}$ and anisotropic components K_i ($i=1$, 2, and 3) as

$$H_{\rm tr}(1,2)=(K_2h_x^2+K_1h_y^2+K_3h_z^2+K_{\rm iso})H_0, \tag{3}$$

$$H_{\rm tr}(3,4)=(K_3h_x^2+K_2h_y^2+K_1h_z^2+K_{\rm iso})H_0, \tag{4}$$

$$H_{\rm tr}(5,6)=(K_1h_x^2+K_3h_y^2+K_2h_z^2+K_{\rm iso})H_0, \tag{5}$$

where $(h_x,h_y,h_z)=\frac{1}{\sqrt{2}}(\sin\theta,\sin\theta,\sqrt{2}\cos\theta)$ is a unit vector along $\mathbf{H}_0$. The principal values of the anisotropic component $K_{\rm i}$ are defined so as to fulfill the relations $K_1+K_2+K_3=0$ and $|K_3|\geq|K_1|\geq|K_2|$. The definitions of $K_{1,2,3}$ at each P site are illustrated in Fig. 1. The equations are valid when there is no magnetic anisotropy in a cubic system. As shown by the solid lines in Fig. 3(c), the calculated curves of Eqs. (3)–(5) give a satisfactory reproduction of the experimental data with $K_{\rm iso}H_0=48$ Oe and $(K_1,K_2,K_3)H_0=(-38,-7,45)$ Oe, respectively.

B. Temperature dependence of the transferred HF interactions

Figure 4 shows the temperature dependence of the isotropic $K_{\rm iso}$ and anisotropic parts of the Knight shift $K_{1,2,3}$. Here, instead of measuring the field-orientation dependence of the ^{31}P-NMR spectra at all the temperatures, the Knight-shift values are extracted by using the equations from Eqs. (3)–(5) for $(h_x,h_y,h_z)=(0,0,1)$, that is,

$$K_{\rm iso}H_0 = \{H_{\rm tr}^{[001]}(1,2) + H_{\rm tr}^{[001]}(3,4) + H_{\rm tr}^{[001]}(5,6)\}/3, \quad (6)$$

and

$$K_1H_0 = H_{\rm tr}^{[001]}(3,4) - K_{\rm iso}H_0, \quad (7)$$

$$K_2H_0 = H_{\rm tr}^{[001]}(5,6) - K_{\rm iso}H_0, \quad (8)$$

$$K_3H_0 = H_{\rm tr}^{[001]}(1,2) - K_{\rm iso}H_0, \quad (9)$$

where $H_{\rm tr}^{[001]} = \Delta H^{[001]} - H_{\rm dip}^{[001]}$ represents the transferred HF field at $\mathbf{H}_0 \| [001]$. In Fig. 4, we have also plotted the $K_{\rm iso}$ estimated from the NMR spectra at $\mathbf{H}_0 \| [111]$ by using the relation

$$K_{\rm iso}H_0 = H_{\rm tr}^{[111]}. \quad (10)$$

As seen in the figure, the estimates from Eqs. (6) and (10) agree with each other above $T \sim 35$ K. The deviation below 35 K is associated with a small anisotropy observed in the bulk magnetization around 50 kOe. As seen in Fig. 4, $K_{\rm iso}$ and K_3 increase, while K_1 and K_2 decrease, as temperature decreases. Therefore, the coupling constant is positive for $K_{\rm iso}$ and K_3 while it is negative for K_1 and K_2.

For f-electron systems in general, the Knight shift is composed of the spin part K^s and the Van Vleck part K^v. These components are connected with the T-dependent spin susceptibility χ^s and the T-independent Van Vleck susceptibility χ^v as

$$K(T) = K^s(T) + K^v = \frac{1}{N_A\mu_B}[A^s\chi^s(T) + A^v\chi^v], \quad (11)$$

where $A^{s(v)}$ is the spin (Van Vleck) part of the isotropic/anisotropic HF coupling constants, N_A is Avogadro's number, and μ_B is the Bohr magneton. K^v is expected to occur particularly in an f electron system where spin and orbital degrees of freedom strongly couple with each other so that the spin operator also contributes to the Van Vleck term.[13,14] In Fig. 5, we plot $K_{\rm iso}$ and $K_{1,2,3}$ against χ with temperature as an implicit parameter. Both $K_{\rm iso}$ and $K_{1,2,3}$ maintain a linear relation with χ except for a small deviation near the ferromagnetic phase boundary below 28 K. The slopes of the K-χ plots yield for the isotropic and anisotropic spin parts of the transferred HF coupling constants $A_{\rm iso}^s$ and (A_1^s, A_2^s, A_3^s) the values 887 Oe/μ_B and $(-510, -491, 1001)$ Oe/μ_B, respectively. On the other hand, the intersections of the linear fits at $\chi = 0$ are almost zero for both $K_{\rm iso}$ and $K_{1,2,3}$, as seen in Fig. 5. This indicates that the Van Vleck contributions $K^v \simeq 0\%$ at the P sites.

The isotropic part of the transferred HF interaction is composed of the Fermi contact and the core-polarization interactions. The former arises from the local spin density in the P 3s orbital while the latter arises from the inner-core polarization effect where the closed inner s electrons are polarized by the unpaired P 3p electrons through an exchange polarization effect. Note that the estimated value of $A_{\rm iso}^s$ is more than two times larger than that in UFe_4P_{12}, which is an insulator. This implies that the Fermi contact interaction, which most likely dominates the positive value of $A_{\rm iso}^s$, is enlarged in semimetallic $NpFe_4P_{12}$ due to the enhancement

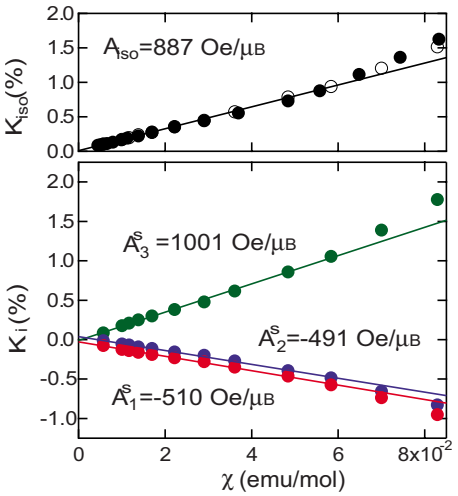

FIG. 5. (Color online) $K_{\rm iso}$ and $K_{1,2,3}$ are plotted against the bulk susceptibility χ with temperature as an implicit parameter. The slopes of the solid lines correspond to the isotropic and anisotropic parts of the HF coupling constants for the spin part $A_{\rm iso}^s = 887$ Oe/μ_B and $(A_1^s, A_2^s, A_3^s) = (-510, -491, 1001)$ Oe/μ_B, respectively.

of the s-f hybridization effect associated with the enhancement of P 3s electron contributions to the conduction band. On the other hand, it should be also noted that the $A_{\rm iso}^s$ value is still much smaller than those for metallic compounds. For example, the value of $|A_{\rm iso}^s| = 84$ kOe/μ_B has been reported for NpP.[15] Therefore, the estimated value of $A_{\rm iso}^s$ is indicative of a relatively small contribution of P 3s electrons to the conduction band.

On the other hand, the anisotropic part of the transferred HF interaction may be attributed to the on-site spin-dipolar interactions from the local spin densities on P 3p orbitals. A_i^s terms are thus related with the local spin densities of three orthogonal 3p orbitals, $f_1, f_2, f_3 (>0)$, as[16,17]

$$\begin{bmatrix} A_1^s \\ A_2^s \\ A_3^s \end{bmatrix} = A_{3p} \begin{bmatrix} 1 & -\frac{1}{2} & -\frac{1}{2} \\ -\frac{1}{2} & 1 & -\frac{1}{2} \\ -\frac{1}{2} & -\frac{1}{2} & 1 \end{bmatrix} \begin{bmatrix} f_1 \\ f_2 \\ f_3 \end{bmatrix}, \quad (12)$$

where $A_{3p} \equiv (4/5)\mu_B\langle r^{-3}\rangle_{3p} \approx 174$ KOe/μ_B for a fully polarized 3p state.[18] From Eq. (12), the local spin densities at each 3p orbital were estimated to be $(f_1, f_2, f_3) \approx (0, 0.007, 0.58)\%$, respectively. The relation, $f_3 \gg f_1, f_2$, indicates that the spin moments are induced mostly on the P 3p orbital extending parallel to K_3, e.g., the 3p_z orbital for the (P1, P2) sites in Fig. 1. Since this orbital extends toward the inside of the P cage where a Np ion is located, one can expect that this orbital will have the largest hybridization effect with Np 5f electrons.

Now we compare our results with previous estimates of the local spin density at the Be 2p orbitals for UBe_{13}.[17] In the latter compound, twelve Be ions form an icosahedral cage

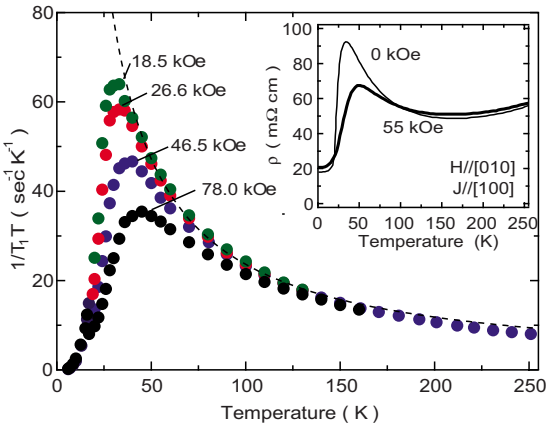

FIG. 6. (Color online) The temperature dependence of $1/T_1T$ measured at fields of 18.5, 26.6, 46.5, and 78.0 kOe ($\|\langle 111\rangle$), respectively. The inset shows the temperature dependence of the resistivity at fields of 0 and 55 kOe (Ref. 3).

similar to that in filled skutterudites while the center of the Be cage is filled by another Be ion, where U ions with $5f$ electrons form a cube surrounding the Be cage. In such a case, the authors found the largest spin density, f_3, on the $2p$ orbital perpendicular to the mirror plane for each Be site [corresponding to the P_y orbital for P(1,2) sites in $NpFe_4P_{12}$]. Furthermore, the f_3 value estimated was $\simeq 4.2\%$. Therefore, the present f_3 value in $NpFe_4P_{12}$ is an order-of-magnitude smaller than that for UBe_{13}. The small f_3 value indicates a weak hybridization effect between P $3p$ and Np $5f$ electrons, which is attributed to a localized character for Np $5f$ electrons in $NpFe_4P_{12}$.

C. Temperature and field dependences of the spin-lattice relaxation rate $1/T_1$

NMR is also a suitable tool for probing low-energy magnetic excitations via nuclear relaxation rates. The spin-lattice relaxation rate $1/T_1$ is related to the low-energy spin-fluctuation densities perpendicular to the quantization axis, and is given by

$$(1/T_1T)_{\|} = \frac{\gamma_n^2 k_B}{2} \sum_q A_{\rm hf}(q)_{\perp}^2 \frac{{\rm Im}\,\chi(q,\omega_n)_{\perp}}{\omega_n}, \qquad (13)$$

where ${\rm Im}\,\chi(q,\omega_n)$ is the dissipative magnetic susceptibility, ω_n is the NMR resonance frequency, and $A_{\rm hf}(\boldsymbol{q})$ is the $\boldsymbol{q}$-dependent hyperfine coupling constant [$A_{\rm hf} \equiv A_{\rm hf}(0)$].

Figure 6 shows the temperature dependence of $1/T_1T$ measured in fields of 18.5, 26.6, 46.5, and 78.0 kOe, respectively. All the data were taken at a lower-frequency peak of the P-NMR spectra with $\mathbf{H}_0\|\langle 111\rangle$. There is a strikingly large field dependence to the measured rates. In the lowest field of 18.5 kOe, $1/T_1T$ increases rapidly with decreasing temperature and shows a broad maximum around $T_{\rm max} \sim 30$ K. With increasing field, however, the increase in $1/T_1T$ is strongly suppressed below 100 K. At the same time, the broad maximum in $1/T_1T$ vs T shifts to higher temperatures, e.g., $T_{\rm max} \sim 50$ K in a field of 78.0 kOe. In all the fields, $1/T_1T$ shows a rapid decrease below $T_{\rm max}$ without a distinguishable anomaly related with the onset of the ferromagnetic ordering around T_C. Instead, we have observed an anomaly around $T^* \sim 19$ K, which will be discussed later.

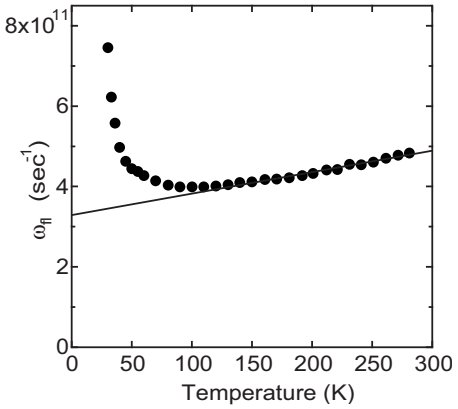

FIG. 7. The temperature dependence of $T_1 \propto \omega_{\rm fl}(T)$ at field of 46.5 kOe. The solid line shows the relation $\omega_{\rm fl}(T) = \alpha + \beta T$.

Let us first characterize the spin fluctuations at temperatures above 100 K, where $1/T_1$ is nearly field independent. In this temperature region well above T_C, the nuclear-spin relaxation can be regarded as being driven by independent fluctuations of the Np local moments. Assuming the dynamical susceptibility to be isotropic and the q dependence of $A(q)$ to be negligible, $1/T_1$ is known to be expressed as follows:[19]

$$1/T_1 = \sqrt{2\pi}(g\gamma_N)^2 A_{\rm hf}^2 \frac{J(J+1)}{3\omega_{\rm fl}}, \qquad (14)$$

where $\omega_{\rm fl}$ is the local-moment fluctuation rate, assumed $\gg \gamma$H, and $A_{\rm hf}$ is the $\boldsymbol{q}$-independent hyperfine coupling constant, i.e., $A_{\rm hf} \simeq (A_{\rm tr}^2 + A_{\rm dip}^2)^{1/2} = 848$ Oe/μ_B for $H_0\|\langle 111\rangle$. In general, $\omega_{\rm fl}$ is given by two major processes, that is, $\omega_{\rm fl} = \omega_{\rm ex} + \omega_{\rm cf}$. The $\omega_{\rm ex}$ represents a fluctuation process caused by the superexchange coupling $J_{\rm ex}$ between Np moments. This $\omega_{\rm ex}$ is denoted by $\omega_{\rm ex}^2 = 2zJ_{\rm ex}^2[J(J+1)]/(3\hbar^2)$ and thus gives a well-known T-independent T_1 process for a fully localized spin system. On the other hand, $\omega_{\rm cf}$ is due to the spin-exchange interactions with conduction electrons and is written as $\omega_{\rm cf} = \frac{\pi}{\hbar}(J_{\rm cf}\rho)^2 k_B T$, where $J_{\rm cf}$ is the spin-exchange coupling between the Np local moments and conduction electrons, ρ is the band density of states, and z is the number of nearest-neighbor moments, i.e., $z=8$ in our case. The $\omega_{\rm cf}$ thus provides a T-linear dependence for T_1.

In Fig. 7, we plot the temperature dependence of $\omega_{\rm fl}$ ($\propto T_1$). As shown by the solid line, $\omega_{\rm fl}$ exhibits a weak T-linear dependence as $\omega_{\rm fl} = \alpha + \beta T$ above 100 K. This indicates that both the $\omega_{\rm ex}$ and $\omega_{\rm cf}$ processes are available for the nuclear relaxation in $NpFe_4P_{12}$. From the constant term α, the superexchange coupling $J_{\rm ex}/k_B$ has been estimated to be ~ 0.22 K, which is in agreement in order of magnitude with $J_{\rm ex}^*/k_B \sim 0.35$ K as expected from mean-field theory for $T_C = 23$ K. On the other hand, from the slope β, we have estimated $J_{\rm cf}\rho \sim 0.025$, which is an order-of-magnitude smaller than the reported value $J_{\rm cf}\rho \sim 0.213$ for $PrFe_4P_{12}$.[20] The present $1/T_1$ analysis shows that the dominant interaction for

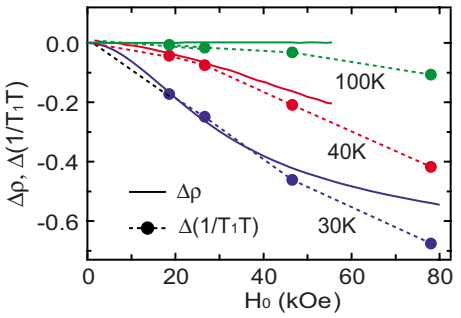

FIG. 8. (Color online) The field dependence of $\Delta\rho$ (solid lines) and $\Delta(1/T_1T)$ (circles) at $T=30$, 40, and 100 K. Here $\Delta\rho$ and $\Delta(1/T_1T)$ are defined as $\Delta\rho=[\rho(H_0)-\rho(0)]/\rho(0)$ and $\Delta 1/T_1T=[1/T_1T(H_0)-1/T_1T(0)]/[1/T_1T(0)]$, respectively.

the Np local moments is their mutual superexchange coupling J_{ex}, which ultimately drives the ferromagnetic ordering below T_C. Meanwhile, as we shall see below, the presence of the spin-exchange coupling J_{cf} is also important and associated with the occurrence of the negative MR in this system.

In the lower temperature region, on the other hand, $1/T_1T$ shows a rapid increase with decreasing temperature and shows a maximum at T_{max} above T_C. In this temperature region, ferromagnetic correlations are developing among local moments so that the low-energy spin fluctuations are enhanced rapidly as the temperature decreases. Because of the ferromagnetically enhanced susceptibility, however, an applied field quickly quenches out the low-energy spin fluctuations, which results in progressive suppression of $1/T_1T$ with increasing field, as seen in Fig. 6. The suppression of $1/T_1T$ has been observed in a wide temperature range of up to 100 K. This reveals that short-range ferromagnetic correlations are developing from relatively high temperatures in $NpFe_4P_{12}$. The rapid decrease in $1/T_1T$ below T_{max} suggests the appearance of field-induced ferromagnetic ordering above T_C.

Note that a large and negative MR has been observed in almost the same temperature region where the field dependent $1/T_1T$ has been observed. The inset to Fig. 6 shows the temperature dependence of the resistivity $\rho(T)$ in fields of 0 and 55 kOe.[3] The resistivity at zero field increases rapidly with decreasing temperature below 150 K. On the other hand, the resistivity at 55 kOe is suppressed, compared with that at zero field, in the temperature range from 100 to 20 K. At the same time, the broad maximum in $\rho(T)$ shifts from ~30 K at zero field to ~50 K at $H_0=55$ kOe. A change in resistance induced by a magnetic field has been found to reach a value as large as ~−60% around 30 K and decays in a wide temperature range of up to about $4T_C$.[3] These characteristics stands in a sharp distinction to negative MR in ordinary metallic ferromagnets.[21,22]

In Fig. 8, we compare the field dependence of $\Delta\rho$ and $\Delta(1/T_1T)$ at $T=30$, 40, and 100 K. Here $\Delta\rho$ and $\Delta(1/T_1T)$ are defined as $\Delta\rho=[\rho(H_0)-\rho(0)]/\rho(0)$ and $\Delta 1/T_1T=[1/T_1T(H_0)-1/T_1T(0)]/[1/T_1T(0)]$, respectively. The values of $1/T_1T(0)$ were deduced by assuming a linear variation for $1/T_1T(H_0)$ below 30 kOe, as shown by the dotted lines in the figure, since zero-field NMR (NQR) is not available for the P ($I=1/2$) nucleus. It is seen that $\Delta\rho$ and $\Delta(1/T_1T)$ show

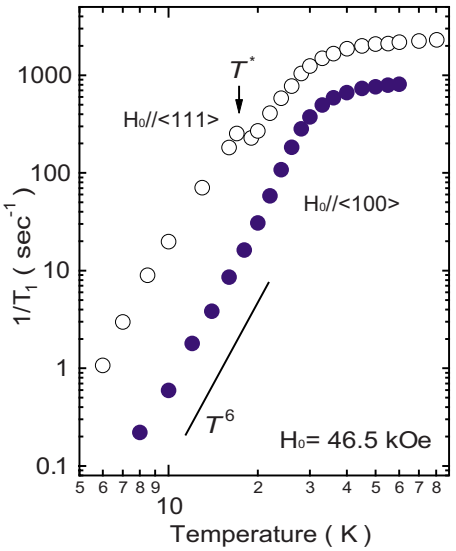

FIG. 9. (Color online) The temperature dependence of $1/T_1$ at low temperatures with the applied field parallel to ⟨111⟩ and ⟨100⟩, respectively.

a similar field dependence, especially in the lower field region below $H_0=40$ kOe. This suggests that the large MR effect over a wide temperature range is closely related to the suppression of low-energy spin fluctuations by an applied field. Although there is no microscopic theory which could explain quantitatively the relation between $\Delta\rho$ and $\Delta(1/T_1T)$ at present, it is expected that the development of short-range ferromagnetic correlations on the scale of the mean-free path would cause rapid suppression of the magnetic scattering as well as the low-energy spin fluctuations. A scattering mechanism associated with magnetic polarons has been proposed recently to explain the large MR effects for ferromagnetic intermetallics URhSi and URhGe.[23]

Finally, we deal with $1/T_1$ at temperatures below T_C. In Fig. 9, we plot the temperature dependence of $1/T_1$ at low temperatures on a log-log scale. In general, the nuclear relaxation in the ordered state is analyzed using the multimagnon scattering theory. In the ferromagnetic case, if the HF interaction is anisotropic, a two-magnon Raman process and a three-magnon process were suggested to induce nuclear-spin flips, and thereby, spin-lattice relaxation.[24,25] These two processes are known to provide characteristic temperature dependences: $1/T_1 \propto T^2$ for the former, and $\propto T^{7/2}$ for the latter. In $NpFe_4P_{12}$, however, we found that $1/T_1$ shows rather strong temperature dependence, i.e., it varies as $1/T_1 \propto T^6$ below 20 K, as shown in Fig. 9. To our knowledge, there is no magnon theory explaining T^6 behavior for $1/T_1$.

With the field applied parallel to ⟨111⟩, we have observed an anomaly in the temperature dependence of $1/T_1$ around $T^* \sim 19$ K. This T^* corresponds to the temperature where the reorientation of the ordered Np moments has been reported.[3,10] Namely, the Np $5f$ moments are ferromagnetically aligned along the applied field above T^* while they are reoriented along the ferromagnetic easy axis of the ⟨100⟩ direction below T^*. This behavior is connected with the temperature dependence of magnetic anisotropy energy. Note that T^* has not been defined when the field is applied parallel

to ⟨100⟩ since the moments are already aligned along the ferromagnetic easy axis at high temperatures. Therefore, as shown in Fig. 9, no anomaly has been observed in $1/T_1$ with $H_0 \| \langle 100 \rangle$.

IV. SUMMARY

The hyperfine interactions and magnetic fluctuations have been investigated in the neptunium-based ferromagnet $NpFe_4P_{12}$. From the angular dependence of the ^{31}P-NMR line splitting, we have obtained the transferred HF interactions at ^{31}P nuclei, and then from their anisotropies, deduced the local spin densities at P $3p$ orbitals. We found that only a small fraction of Np $5f$ orbital character is admixed into the P $3p$ orbitals extending toward the inside of the P cage where a Np ion is located. The weak hybridization effect between Np $5f$ and P $3p$ orbitals indicates localized character for the Np $5f$ electrons in $NpFe_4P_{12}$.

We also conducted an analysis of $1/T_1$ on the basis of a localized picture for the Np $5f$ electrons. This analysis reveals that the dominant interaction for the Np spin moments is their mutual superexchange coupling J_{ex}. In addition, we found that an applied field very quickly quenches out the low-energy spin fluctuations of Np $5f$ spin moments, having the effect of suppressing the T_1 process in a wide temperature range up to 4 T_C. This finding led us to suggest that the large and negative MR observed in the same temperature range comes from the reduction in the magnetic scattering from Np $5f$ spin moments by an applied field.

ACKNOWLEDGMENTS

We would like to thank R. E. Walstedt for valuable discussions. This work was supported by a Grant-in-Aid for Scientific Research of The Ministry of Education, Culture, Sports, Science, and Technology, Japan.

*tokunaga.yo@jaea.go.jp
†Present address: DRFMC/SPSMS, CEA-Grenoble, Grenoble 38054, France

[1] See, for example, M. B. Maple, P.-C. Ho, V. S. Zapf, N. A. Frederick, E. D. Bauer, W. M. Yuhasz, F. M. Woodward, and J. W. Lynn, J. Phys. Soc. Jpn. Suppl. A **71**, 23 (2002).
[2] See, for example, H. Sato, Y. Aoki, T. Namiki, T. D. Matsuda, K. Abe, S. Osaki, S. R. Saha, and H. Sugawara, Physica B **328**, 34 (2003); H. Sato, D. Kikuchi, K. Tanaka, H. Aoki, K. Kuwahara, Y. Aoki, M. Kohgi, H. Sugawara, and K. Iwasa, J. Magn. Magn. Mater. **310**, 188 (2007).
[3] D. Aoki, Y. Haga, Y. Homma, H. Sakai, S. Ikeda, Y. Shiokawa, E. Yamamoto, A. Nakamura, and Y. Ōnuki, J. Phys. Soc. Jpn. **75**, 073703 (2006).
[4] G. P. Meisner, M. S. Torikachvili, K. N. Yang, M. B. Maple, and R. P. Guertin, J. Appl. Phys. **57**, 3073 (1985).
[5] M. S. Torikachvili, C. Rossel, M. W. McElfresh, M. B. Maple, R. P. Guertin, and G. P. Meisner, J. Magn. Magn. Mater. **54-57**, 365 (1986).
[6] T. D. Matsuda, A. Galatanu, Y. Haga, S. Ikeda, E. Yamamoto, M. Hedo, Y. Uwatoko, T. Takeuchi, K. Sugiyama, K. Kindo, R. Settai, and Y. Ōnuki, J. Phys. Soc. Jpn. **73**, 2533 (2004).
[7] M. S. Torikachvili, J. W. Chen, Y. Dalichaouch, R. P. Guertin, M. W. McElfresh, C. Rossel, M. B. Maple, and G. P. Meisner, Phys. Rev. B **36**, 8660 (1987).
[8] H. Sato, Y. Abe, H. Okada, T. D. Matsuda, K. Abe, H. Sugawara, and Y. Aoki, Phys. Rev. B **62**, 15125 (2000).
[9] H. Sato, Y. Abe, T. D. Matsuda, K. Abe, T. Namiki, H. Sugawara, and Y. Aoki, J. Magn. Magn. Mater. **258-259**, 67 (2003).
[10] Y. Tokunaga, D. Aoki, Y. Homma, H. Sakai, H. Chudo, S. Kambe, T. D. Matsuda, S. Ikeda, E. Yamamoto, A. Nakamura, Y. Haga, Y. Shiokawa, Y. Ōnuki, and H. Yasuoka, J. Phys. Soc. Jpn. Suppl. **77**, 211 (2008).
[11] Y. Tokunaga, T. D. Matsuda, H. Sakai, H. Kato, S. Kambe, R. E. Walstedt, Y. Haga, Y. Ōnuki, and H. Yasuoka, Phys. Rev. B **71**, 045124 (2005).
[12] J. Kikuchi, M. Takigawa, H. Sugawara, and H. Sato, J. Phys. Soc. Jpn. **76**, 043705 (2007).
[13] T. Ohama, H. Yasuoka, D. Mandrus, Z. Fisk, and J. L. Smith, J. Phys. Soc. Jpn. **64**, 2628 (1995).
[14] H. Kato, H. Sakai, Y. Tokunaga, Y. Tokiwa, S. Ikeda, Y. Ōnuki, S. Kambe, and R. E. Walstedt, J. Phys. Soc. Jpn. **72**, 2357 (2003).
[15] D. J. Lam and F. Y. Fradin, Phys. Rev. B **9**, 238 (1974).
[16] A. Abragam, *The Principles of Nuclear Magnetism* (Oxford University Press, Oxford, 1961), Chap. VI.
[17] H. Tou, N. Tsugawa, M. Sera, H. Harima, Y. Haga, and Y. Ōnuki, J. Phys. Soc. Jpn. **76**, 024705 (2007).
[18] R. G. Barnes and W. V. Smith, Phys. Rev. **93**, 95 (1954).
[19] T. Moriya, Prog. Theor. Phys. **16**, 641 (1956).
[20] K. Ishida, H. Murakawa, K. Kitagawa, Y. Ihara, H. Kotegawa, M. Yogi, Y. Kitaoka, Ben-Li Young, M. S. Rose, D. E. MacLaughlin, H. Sugawara, T. D. Matsuda, Y. Aoki, H. Sato, and H. Harima, Phys. Rev. B **71**, 024424 (2005).
[21] H. Yamada and S. Takada, Prog. Theor. Phys. **49**, 1401 (1973); J. Phys. Soc. Jpn. **34**, 51 (1973).
[22] K. Ueda, Solid State Commun. **19**, 965 (1976).
[23] V. H. Tran and R. Troć, Phys. Rev. B **57**, 11592 (1998).
[24] T. Oguchi and F. Keffer, J. Phys. Chem. Solids **25**, 405 (1964).
[25] D. Beeman and P. Pincus, Phys. Rev. **166**, 359 (1968).